Building Tomorrow's Society
Bâtir la Société de Demain

Fredericton, Canada
June 13 – June 16, 2018/ *Juin 13 – Juin 16, 2018*

CURVATURE DUCTILITY OF CONCRETE COLUMNS WITH LOW AXIAL LOADS

van Weerdhuizen, M.[1,2], and Bartlett, F.M.[1]
[1] University of Western Ontario, Canada
[2] mvanweer@uwo.ca

Abstract: Quantification of curvature ductility in concrete columns provides a basis for more accurately describing the warning of failure of a structural element. Curvature ductility, defined as the ratio of ultimate curvature to yield curvature, is a metric for warning of failure. In this study, cross sections having total reinforcing ratios ranging from 0.01 to 0.04, normalized spacing of outermost reinforcing layers, γ, ranging from 0.6 to 0.9, and concrete strengths ranging from 25 to 50 MPa are considered. Using typical idealizations for ultimate and yield moment calculations, cross sections were analyzed under a range of axial forces. The maximum axial load was taken as that corresponding to the balance point, where concrete crushing and steel yielding occur simultaneously. Curvatures at ultimate and yield limit states for each combination of parameters were used to form generalized equations for ductility ratios using multiple linear regression. Response-2000 analysis of an array of cross sections was used to validate the results independently. The generalized equations were found to be consistent lower bounds to the Response-2000 results. Curvature ductility ratios from one to twenty-five were observed over the parameter ranges considered. High ductility was observed for low axial loads, where behavior approached that of a beam in pure bending. Maximum ductility was achieved when the lever arm created by the outermost layers of reinforcement was large and the reinforcing ratio was small. Curvature ductility decreased with greater axial loads. Trends in observed ductility ratios allowed the warning of cross-section failure to be quantified using the basic parameters investigated.

1 INTRODUCTION

When designing and assessing structures, nominal probabilities of failure may be expressed using reliability indices [e.g. Canadian Standards Association 1981, Construction Industry Research and Information Association 1977]. The acceptable probability of failure depends on the consequences of a potential collapse with respect to the life safety of the occupants and therefore on the warning of structural failure provided. These considerations are captured by the structural redundancy and ductility of the cross section, which relate to reliability methods as outlined in Figure 1.

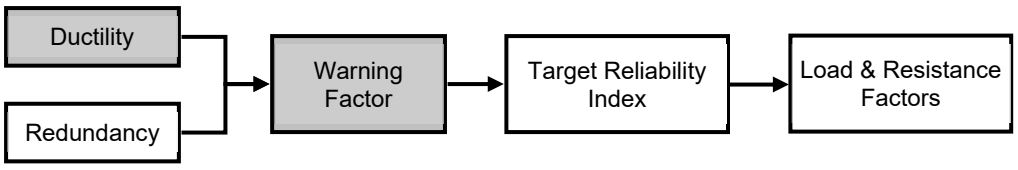

Figure 1: Reliability methods concept map

The present research focuses on the ductility aspect of warning factor, and subsequent study will investigate the influence of redundant structural systems. Current methods use reliability indices to provide the user with prescribed factored load combinations, using the resistance factors associated with new

design. The target reliability index is defined as $\beta_T = -\Phi^{-1}(P_f)$, where P_f is the nominal probability of failure, and Φ is the standard normal distribution. The target probability of failure can be expressed as a function of the number of people at risk, n, and the warning of failure, w:

$$[1] \quad P_f = \frac{Ak}{w\sqrt{n}}$$

where A is an activity factor specific to the type of structure being assessed, and k is a calibration factor (10^{-4}) (Canadian Standards Association, 1981).

For the assessment of an element in an existing structure, a target reliability index may be assigned that is different from that used for the design of a new structure. For an existing element, an assessment of the structure provides information about the element under consideration, and the structure as a whole. The cross-sectional and material properties may be known with a degree of relative certainty compared to those for structures in the design phase. Therefore, a target reliability index may be selected that accounts for the actual field conditions, which may then correspond to more or less stringent requirements than those associated with the design of an equivalent new element.

Several methods to assign target reliability indices have been developed for use in design and assessment. CSA S408-81 (1981) outlines the theory behind the application of warning factor concepts to probability of failure calculations. CIRIA Report 63 (Construction Industry Research and Information Association, 1977) provides a similar definition for probability of failure, without the explicit consideration of a warning factor; instead it proposes the use of a combination of a social criterion factor, K_s, and the design life of the structure, n_d.

Allen (1991), and the provisions in the National Building Code of Canada Commentary L (2010) developed subsequently, use a set of additive components to provide a target “reliability level”. These correspond to load factors to be used in the assessment procedure to determine the structural demand. Similarly, in Allen (1992) and CSA S6-06 (2006), load factors are selected based on a target reliability index. Here, target reliability indices are quantified based on traffic type, inspection level, system behaviour, and element behaviour.

A drawback of methods formulated in this way is that they use discrete categories for warning factors. The categories lack quantifiable criteria for classifying elements, which introduces inconsistency in how the provisions are applied. Additional concerns arise due to the application of target reliability concepts to the factored demand rather than the factored resistance. Consequently, each load combination must be checked separately, while material-specific effects are ignored. In design codes, partial resistance factors have been calibrated to empirical statistical data, whereas for assessment, material and cross-sectional parameters can be field measured and used for calibration of element-specific resistance factors.

Figure 2 shows the moment-curvature responses obtained from Response-2000 (Bentz & Collins, 2001) for a test cross section under varying axial loads. These illustrate the variability of ductility with axial load. Curve 1, with a normalized axial load of $0.30bhf'_c$, reaches the largest maximum moment, but then quickly fails. Curve 3 shows a much more ductile response but reaches a markedly smaller maximum moment. It is therefore necessary to formulate a procedure to quantify these differences and so derive more appropriate target reliability indices for assessment of reinforced concrete structures.

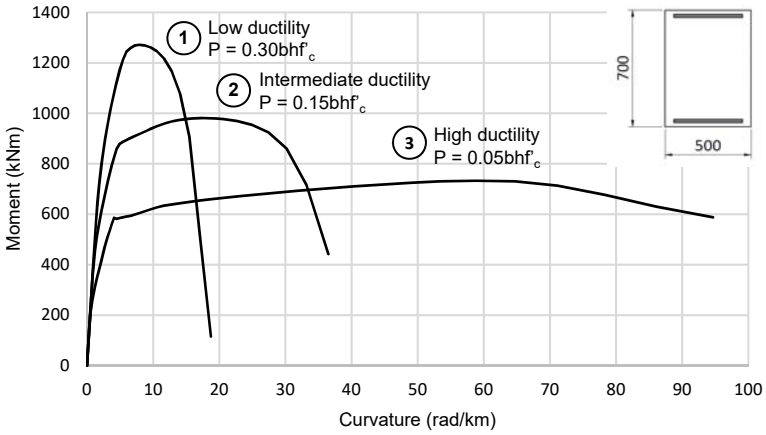

Figure 2: Moment-curvature responses for column cross sections with γ = 0.9, ρ = 0.01

2 PROCEDURE

A standard cross section with dimensions as shown in Figure 3(a) was used as the basis of the analysis. Sections investigated here are identified by their total reinforcing steel ratios, ρ_T, normalized spacing of outermost reinforcing layers, γ, and concrete strength, f'_c. The total reinforcing ratio is defined as $A_s/(bd)$ where A_s is the total area of longitudinal reinforcing in the cross section, equally divided between the top and bottom faces, and b and d are the width and effective depth of the section, respectively. The range of ρ_T is 0.01 to 0.04, representing a practical range of reinforcing for a column as per CSA A23.3 (Canadian Standards Association, 2014). The range of γ for this study was taken to be 0.6 to 0.9, and the range of f'_c taken to be 25 to 50 MPa, representing a general range for commonly designed sections. Columns considered here will be subjected to a combination of flexure and relatively small compressive axial loads where the capacity of the member is governed by the yielding of the tension reinforcing. This implies axial loads ranging from zero to approximately $0.35bhf'_c$.

Each section was analyzed at two resisting moment levels, corresponding to the tension steel reaching its yield strain, and the concrete reaching its crushing strain. These two states are referred to as the Yield Limit State (YLS) and the Ultimate Limit State (ULS), respectively. Stress and strain diagrams for each state are shown in Figure 3. For the purposes of this study, yield strain, ε_y, is assumed to be 0.002 and concrete crushing strain, ε_{cu}, to be 0.0035. Axial load was kept constant at both limit states, allowing comparison of ductility on the basis of normalized applied axial load.

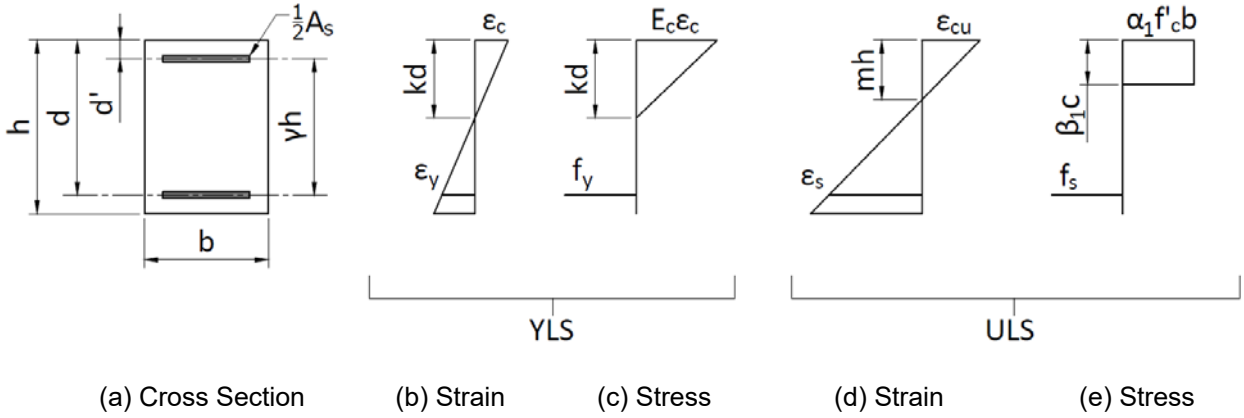

Figure 3: Cross section dimensions, stress and strain diagrams at yield and ultimate limit states

Axial loads and bending moments were calculated using these idealized stress-strain conditions and common assumptions of material and cross section behaviour. All forces and moments were normalized to provide a unitless representation of their magnitudes for the range of cross section parameters investigated.

Figure 3(b) shows the neutral axis depth, kd, when tension reinforcement reaches yield while Figure 3(d) shows mh, the neutral axis depth when concrete begins crushing, which is commonly represented as c. The limits of the value of k are determined by strain limits assumed for the ultimate strength of concrete. A strain limit of 0.002 corresponds to both the maximum, not ultimate, stress in concrete and the yield stress in steel. For these strains, k = 0.64 is implied. Practically, this limit is difficult to achieve, and an upper limit of k = 0.5 was used for data generation. Although compression reinforcement is shown in Figure 3, it is neglected in the simplified analyses presented below.

At YLS, a triangular stress distribution is assumed for concrete in compression, and the axial force may be calculated using stresses as shown in Figure 3(c). At ULS, the concrete stress distribution is assumed to be rectangular, with parameters α_1 and β_1 as shown in Figure 3(e).

The curvature ductility ratio is defined as φ_u/φ_y, where the curvatures, φ, at YLS and ULS are, respectively:

$$[2] \quad \varphi_y = \frac{2\varepsilon_y}{(1+\gamma)(1-k)h}$$

$$[3] \quad \varphi_u = \frac{\varepsilon_{cu}}{mh}$$

Stress and strain distributions at yield, as shown in Figure 3(b) and (c), were used to derive the following equations for normalized axial load, $P/(bhf'_c)$ and moment, $M/(bh^2f'_c)$:

$$[4] \quad \frac{P}{bhf'_c} = \frac{1}{4}\frac{E_c}{f'_c}\varepsilon_y(1+\gamma)\frac{k^2}{1-k} + \frac{1}{4}\frac{f_y}{f'_c}(1+\gamma)\,\rho_T\left[\frac{k(1+\gamma)-1+\gamma}{(1+\gamma)(1-k)}-1\right]$$

$$[5] \quad \frac{M}{bh^2f'_c} = \frac{1}{8}\frac{E_c}{f'_c}\varepsilon_y(1+\gamma)\frac{k^2}{1-k}\left[1-\frac{1}{3}\,k(1+\gamma)\right] + \frac{1}{8}\frac{f_y}{f'_c}(1+\gamma)\,\rho_T\gamma\left[1+\frac{k(1+\gamma)-1+\gamma}{(1+\gamma)(1-k)}\right]$$

Similarly, Equations 6 and 7 were formulated based on stress and strain distributions at the ultimate limit state as shown in Figure 3(d) and (e):

$$[6] \quad \frac{P}{bhf'_c} = a_0\alpha_1\beta_1 m + \frac{1}{4}a_1\rho_T(1+\gamma)\frac{E_s}{f'_c}$$

$$[7] \quad \frac{M}{bh^2f'_c} = \frac{1}{2}b_0\alpha_1\beta_1 m + \frac{1}{8}b_1\rho_T\gamma(1+y)\frac{E_s}{f'_c}$$

Coefficients a_0, a_1, b_0, and b_1 are defined in Table 1 and account for the specific location of the neutral axis, since for some values of γ the compression steel acts in tension.

Table 1: Coefficients for ultimate limit state equations

Range of m	a_0	a_1	b_0	b_1
$\frac{7}{22}(1-\gamma) < m < \frac{7}{6}(1-\gamma)$	1	$\varepsilon_{cu}(1 - \frac{1-\gamma}{2m}) - \varepsilon_y$	$1 - \beta_1 m$	$\varepsilon_y - \varepsilon_{cu}\left(\frac{1-\gamma}{2m}-1\right)$
$\frac{7}{6}(1-\gamma) < m < \frac{1}{2}$	1	0	$1 - \beta_1 m$	$2\varepsilon_y$

The selection of incremental values of k provided the starting point for generation of axial load and bending moment data over a range of axial loads. The value of normalized axial load for each was used in an iterative solution procedure to obtain a corresponding value of m, and thus the moment at ULS.

3 ANALYSIS OF DERIVED CURVATURE DUCTILITY RATIOS

Figure 4 shows the relationship between normalized axial load and curvature ductility ratios for the generated data for several concrete strengths. Sections with extreme values for both ρ_T and γ are shown in the four subfigures.

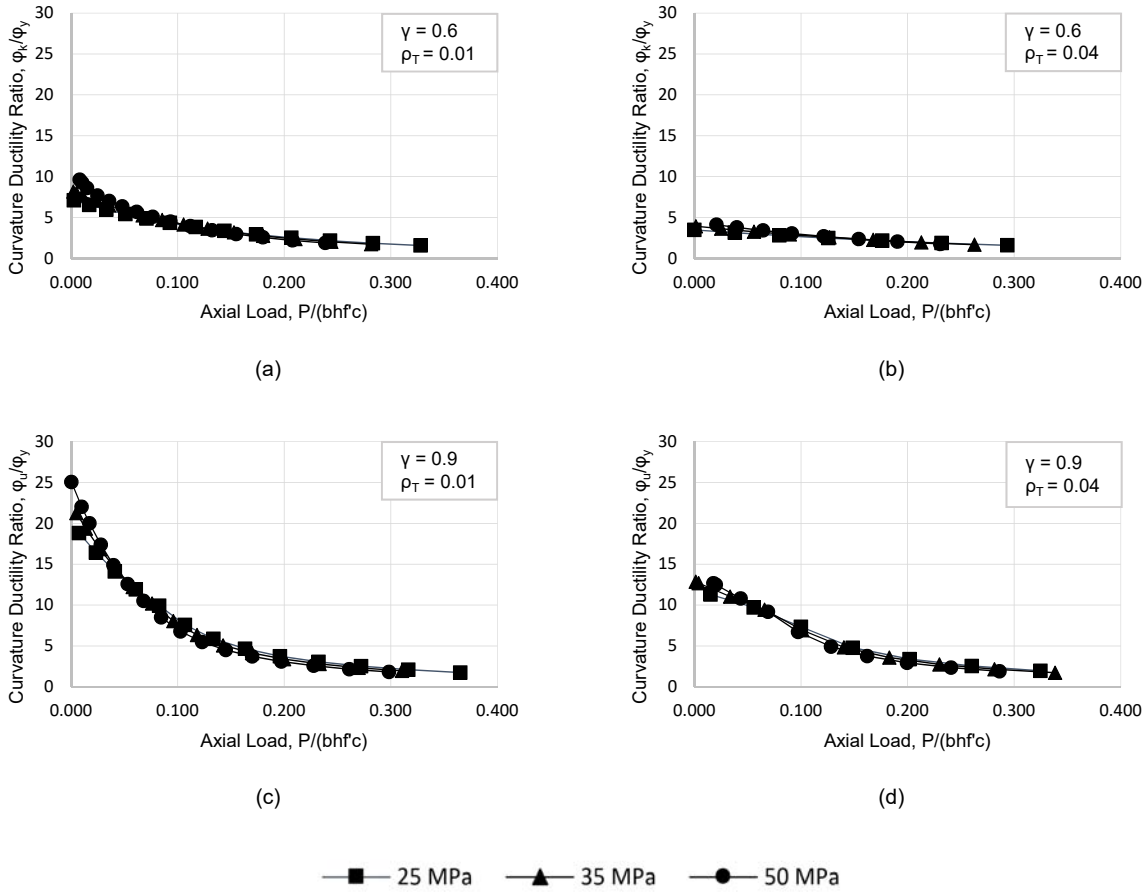

Figure 4: Curvature ductility ratio vs. axial load for various f'c: (a) γ = 0.6, ρ = 0.01; (b) γ = 0.6, ρ = 0.04; (c) γ = 0.9, ρ = 0.01; (d) γ = 0.9, ρ = 0.04.

Figure 4(a) and (c), with data where ρ_T = 0.01, illustrate the considerable impact that varying γ has on curvature ductility ratios. Increasing γ from 0.6 to 0.9 results in maximum ductility ratios in the range of 5 to

10 increasing to a range of 18 to 25. A similar but less pronounced trend can be observed in Figure 4(b) and (d), where $\rho_T = 0.04$. The effects of varying f'_c are relatively small in comparison to varying either ρ or γ. As axial load increases, the variation with f'_c becomes less for all geometries. For this reason, variations in f'_c were neglected in further analysis. Unless noted otherwise, subsequent comparisons will use $f'_c = 25$ MPa, which represents a lower bound of the data set.

Figure 5 shows variation of the ductility ratio with reinforcement ratio for the extreme values of normalized spacing and $f'_c = 25$ MPa. The variability is small relative to the magnitude of the ductility ratio and decreases as axial load approaches its maximum magnitude. The effects of varying the reinforcement ratio are most apparent for low axial loads where steel strains are large and yielding of the reinforcement dictates the behaviour of the cross section. For larger axial loads, the deformation of the steel in tension is considerably smaller and the behaviour of the cross section is more influenced by the concrete acting in compression.

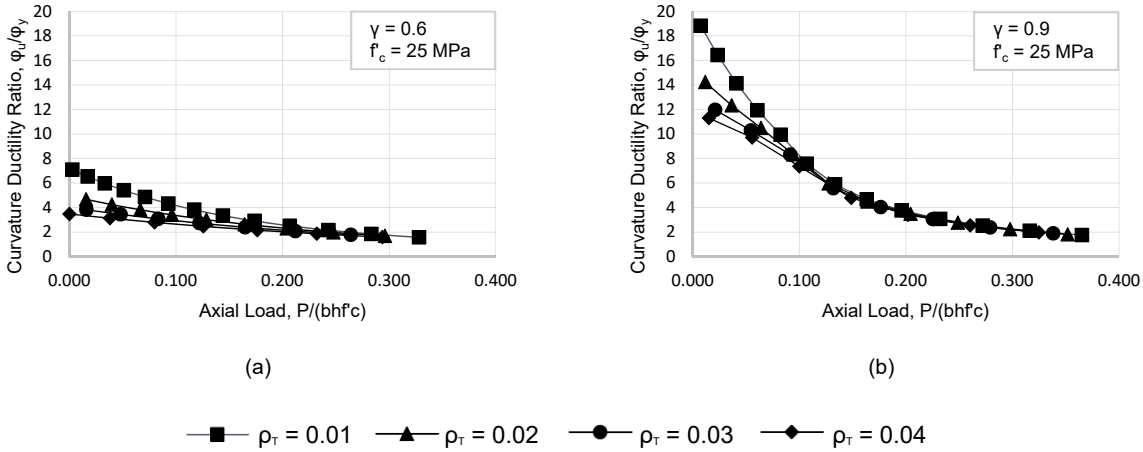

Figure 5: Curvature ductility ratios for various reinforcement ratios: (a) $\gamma = 0.6$; (b) $\gamma = 0.9$.

Similarly, Figure 6 shows the variation of ductility with normalized spacing for given values of reinforcement ratio. For low axial loads, the ductility ratio varies widely with γ, and gives maximum ductility ratios for sections having the largest normalized spacing ($\gamma = 0.9$). As axial load increases, the effects of varying γ diminish over the entire range of reinforcement ratios. Comparing Figures 5 and 6 indicates that the ductility ratio is more sensitive to the spacing of reinforcement than it is to the reinforcement ratio, especially when low axial loads lead to beam-like responses.

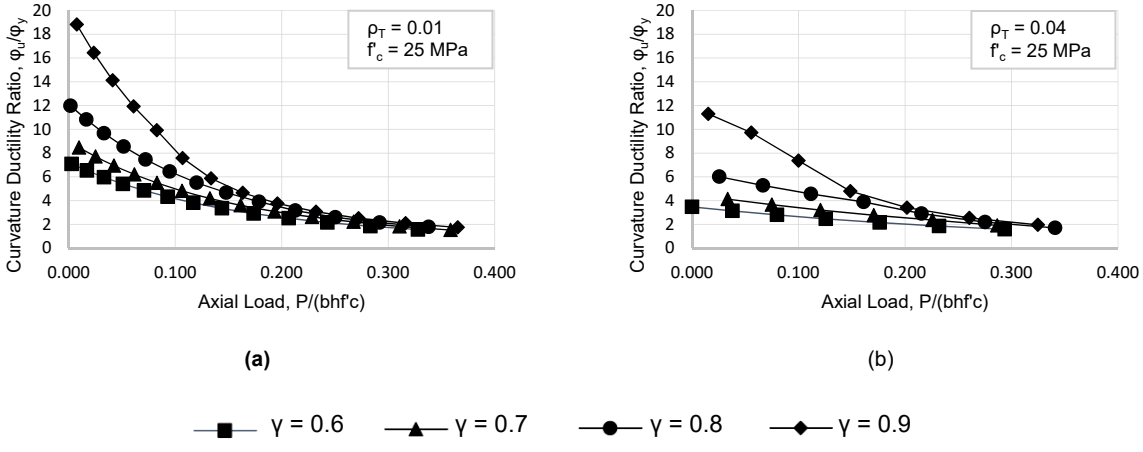

Figure 6: Curvature ductility ratios for various reinforcement spacings: (a) $\rho_T = 0.01$; (b) $\rho_T = 0.04$.

Figure 7 shows four sets of data for γ = 0.9 with reinforcing ratios of 0.01 and 0.04 and concrete strengths of 25 and 50 MPa. Since the variations due to these factors are small when curvature ductility ratios are low, one curve fitted by least squares analysis to data with $\varphi_u/\varphi_y \leq 10$ will be used to represent all sections with γ = 0.9. Based on curves fitted to each individual data set, a generalized curve was created to represent an approximate lower bound of curvature ductility as a function of normalized axial load in this region. For γ = 0.6, the variation with ρ_T is more apparent, so similar curves were fit to data for both ρ_T = 0.01 and ρ_T = 0.04, allowing for interpolation of intermediate values.

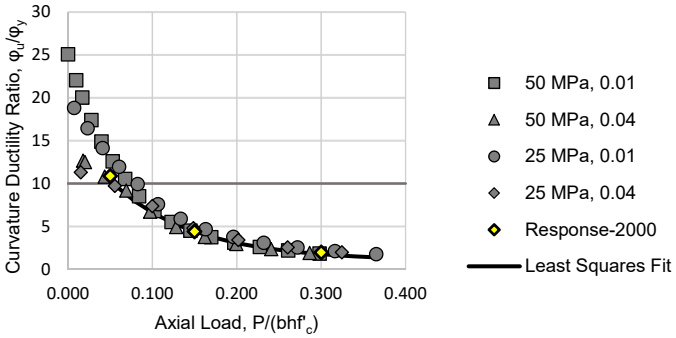

Figure 7: Range-representative data and Response-2000 comparison for γ = 0.9

Response-2000 (Bentz & Collins, 2001) was used to investigate the validity of the results from the idealized analysis. Figure 7 shows data from Reponse-2000 for the cross section presented in Figure 2 with γ = 0.9, ρ_T = 0.01 and f'_c = 35 MPa for three magnitudes of axial load. Response-2000 results indicate ductility ratios consistent with the idealized analysis results.

4 DERIVATION OF WARNING FACTORS

The fitted relationships obtained between ductility ratios and axial load must be transformed into warning factors ranging from zero to one. Previously, these have been defined as discrete values for elements assumed to fall into a number of categories of behaviour. A primary goal of redefining warning factors is to provide a continuous function, avoiding bins, or step functions, where arbitrary discontinuities exist.

Figure 8 illustrates the proposed concept for warning factor definition. As the curvature ductility increases, the warning factor must also increase. A warning factor of one corresponds to high ductility, the definition of which has not previously been well defined. Here, high ductility will be identified as an element with a curvature ductility ratio greater than or equal to ten. A warning factor approaching zero indicates a brittle failure mode, where the curvature at ULS is approximately equal to that at YLS, or $\varphi_u/\varphi_y \approx 1.0$. This definition of warning factor is opposite to that used in the references above, where w = 1.0 corresponds to negligible ductility. Equation 1 will therefore be modified to:

$$[8] \quad P_f = \frac{Akw}{\sqrt{n}}$$

Reversing the scale for w creates a system where a benefit, namely increased warning of failure, corresponds to a positive change in the parameter value. While this definition of w has the advantage of producing a finite value of P_f as the warning factor approaches zero, a non-zero lower limit should be assigned to prevent a target probability of failure equal to zero. A lower limit, close to zero, shall be selected based on the calibration of target reliability indices given the finalized assessment provisions.

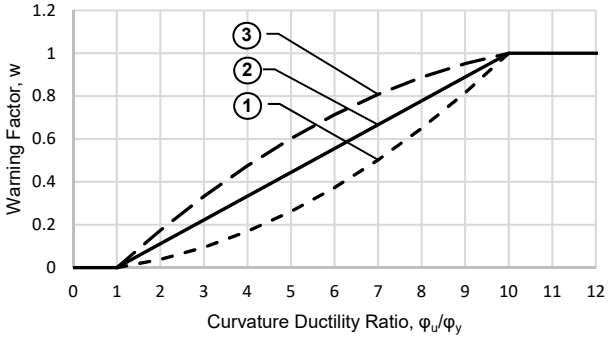

Figure 8: Warning factor-ductility ratio relationship

Figure 8 shows possible transitional relationships, where w = 0 when $\varphi_u/\varphi_y \leq 1.0$ and w = 1.0 when $\varphi_u/\varphi_y \geq 10$. For ductility ratios between these limits, Curves (1), (2), and (3) show positive curvature, linearity, and negative curvature, respectively, in the transition region. Logically, Curve (1) can be deemed inappropriate because of its slope discontinuity at w = 1.0. Curve (3) provides estimates that are the least conservative and is more complicated for users to interpret. The linear relationship expressed by Curve (2) provides a balance of simplicity, conservativism, and smooth transitions. Therefore, all subsequent figures use the following equation for the determination of w:

$$[9] \quad w = \begin{cases} 0^{*}, & \frac{\varphi_u}{\varphi_y} \leq 1.0 \\ \frac{1}{9}\left(\frac{\varphi_u}{\varphi_y} - 1\right), & 1.0 < \frac{\varphi_u}{\varphi_y} < 10 \\ 1, & \frac{\varphi_u}{\varphi_y} \geq 10 \end{cases}$$

*Nominal value equal to zero.

Figure 9 shows the variation of warning factor with normalized axial load derived using Equation 9 to transform data from the fitted curves such as that shown in Figure 7. Warning factors for intermediate values of ρ_T and γ may be obtained by interpolation. The region where w is greater than one is shown for purposes of interpolation only; any cross sections indicating a warning factor greater than one are confined by this upper limit. The enforcement of an upper limit implies that there is a point at which additional ductility is will not provide additional warning.

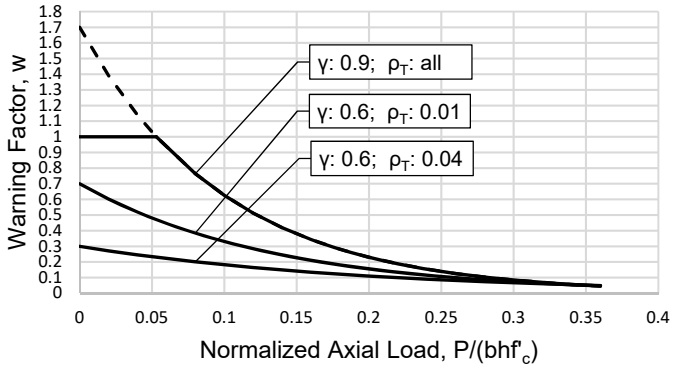

Figure 9: Warning factor selection curves for interpolation

Example. Applying the relationships shown in Figure 9 to the cross sections represented in Figure 2 illustrates the range of w for such widely varying ductilities. The associated warning factors are shown in Table 2. As expected, the moment-curvature response for the lowest axial load is markedly more ductile than the others and therefore results in the highest warning factor.

Table 2: Sample warning factors

Cross Section	Axial Load	φ_u/φ_y	w
1	0.30bhf'c	1.96	0.11
2	0.15bhf'c	4.41	0.38
3	0.05bhf'c	10.88	1.00

5 CONCLUSIONS

The curvature ductility ratio is a useful measure to quantify warning of failure. As axial load increases, the ratio of ultimate to yield curvature decreases, approaching a lower limit of one for all cross sections. Warning factors can be assumed to correlate linearly with ductility ratios within the transitional range from one to ten. Interpolation allows the selection of warning factors based on the cross-section properties. In the low axial load range, where ductility is most sensitive to cross section parameters, interpolated warning factors may be limited by the upper-bound value of one. In regions of relatively high axial loads, warning factors converge, approaching zero and indicating a brittle failure mode.

Acknowledgements

Funding from the Natural Sciences and Engineering Research Council (NSERC) is gratefully acknowledged.

References

Allen, D. E. (1991). Limit states criteria for structural evaluation of existing buildings. *Canadian Journal of Civil Engineering*, 995-1004.

Allen, D. E. (1992). Canadian highway bridge evaluation: reliability index. *Canadian Journal of Civil Engineering*, 987-991.

Bentz, E. C., & Collins, M. P. (2001). *Repsonse-2000 User Manual.* Toronto, ON: University of Toronto.

Canadian Standards Association. (1981). *CAN/CSA S408-81 Guideline for the development of limit states design.* Ottawa, ON: Canadian Standards Association.

Canadian Standards Association. (2006). *CAN/CSA-S6-06, Canadian Highway Bridge Design Code.* Mississauga, ON: Canadian Standards Association.

Canadian Standards Association. (2014). *CSA A23.3-14, Design of concrete structures .* Mississauga, ON: Canadian Standards Association.

Construction Industry Research and Information Association. (1977). *Rationalisation of safety and serviceability factors in structural codes.* London: Construction Industry Research and Information Association.

National Research Council Canada. (2010). Commentary L. In *User's Guide - NBC 2010 Structural Commentaries (Part 4 of Division B)* (pp. L-1 - L-11). Ottawa, ON: National Research Council Canada.